IEEE Access
Multidisciplinary | Rapid Review | Open Access Journal

Received December 4, 2019, accepted December 18, 2019, date of publication December 23, 2019, date of current version January 2, 2020.

Digital Object Identifier 10.1109/ACCESS.2019.2961751

$MoSe_2$-Au Based Sensitivity Enhanced Optical Fiber Surface Plasmon Resonance Biosensor for Detection of Goat-Anti-Rabbit IgG

KUN LIU, JIAHANG ZHANG, JUNFENG JIANG, TIANHUA XU, SHUANG WANG, PENGXIANG CHANG, ZHAO ZHANG, JINYING MA, AND TIEGEN LIU

School of Precision Instruments and Opto-Electronics Engineering, Tianjin University, Tianjin 300072, China
Key Laboratory of Opto-Electronics Information Technology, Ministry of Education, Tianjin 300072, China
Tianjin Optical Fiber Sensing Engineering Center, Institute of Optical Fiber Sensing of Tianjin University, Tianjin 300072, China

Corresponding authors: Kun Liu (beiyangkl@tju.edu.cn) and Junfeng Jiang (jiangjfjxu@tju.edu.cn)

This work was supported in part by the National Natural Science Foundation of China under Grant 61922061, Grant 61775161, and Grant 61775011, and in part by the National Instrument Program under Grant 2013YQ030915.

ABSTRACT Surface Plasmon resonance (SPR) provides an efficacious and label-free detection method for optical fiber bio-sensing. $MoSe_2$ is one of the transition metal dichalcogenides (TMDCs) which has broad applications in detecting specific reactions. Cysteamine hydrochloride with enriched groups can generate self-assemble films for tight attachment. In this study we aimed to combine the rapid response of optical fiber SPR sensors with the enhanced sensitivity of $MoSe_2$ nano-films. An optical fiber SPR biosensor with $MoSe_2$-Au nanostructure was proposed and implemented, and a sensitivity of 2821.81 nm/RIU was achieved, which was approximately 98.7% higher than that of conventional SPR sensor without using $MoSe_2$ nanostructure. Furthermore, Bovine Serum Albumin (BSA) was utilized as the target molecule to test the bioaffinity of the biosensor with $MoSe_2$ deposition cycles from 0 to 8. Weighing the sensitivity and the figure of merit (FOM), the best deposition cycle of $MoSe_2$ was 4 with the sensitivity of 2793.36 nm/RIU and FOM of 37.24 RIU^{-1}. At last, immunization experiments were carried out using Goat-anti-Rabbit IgG and a detection limit of 0.33 μg/mL was achieved. The rapid response and the high bioaffinity showed a strong applicability of the proposed $MoSe_2$-Au SPR immune-sensor in specific interactions and immunization therapy.

INDEX TERMS Surface plasmon resonance, optical fiber, $MoSe_2$, biosensor, Goat-anti-Rabbit IgG.

I. INTRODUCTION

Surface Plasmon resonance (SPR) sensors have attracted much attention due to their real-time and rapid response for the detection of specific molecular interactions and the clinical diagnosis of disease [1]–[3]. In contrast to the traditional prism structures with large size and complex operation, optical fibers exhibit superiorities in the miniaturization, the cost efficiency and the immunity to electromagnetic interferences. Optical fiber SPR biosensors obtained wide applications including the new dual-core D-shaped photonic crystal fiber SPR biosensor for the detection of human blood [4], CFCs (Chlorofluorocarbons), HCFCs (Hydro-Chlorofluorocarbons) [5], salinity and temperature of water substances [6]. The D-type optical fiber SPR biosensor was designed and simulated with a high sensitivity of 66666.67 nm/RIU [7]. Nevertheless, the existing optical fiber SPR sensors face a big challenge in sensitivity. Effective methods for enhancing the sensitivity can be divided into two categories [8], [9]: one is to optimize the internal structure of optical fiber, the other is to involve various sensitivity-improved materials.

The transition-metal dichalcogenides (TMDCs), regarded as another type of super materials after graphene, have drawn considerable attention due to their distinctive optical and electrical characteristics [10]. The TMDCs family includes the compounds e.g. the transition metal elements from group IV to group VII and the chalcogen such as S, Se and Te [11]. Some prism-structure SPR sensors modified using TMDCs materials have been reported. Rahman et al. proposed a sensitivity enhanced sensor structure by adding MoS_2 material in the middle of the Graphene-Au layer on the K9 glass [12].

The associate editor coordinating the review of this manuscript and approving it for publication was Sukhdev Roy.

A sensitivity of 2524.8 nm/RIU was achieved with $MoSe_2$ suspension on the Kretschmann structure. Compared to the case without using any $MoSe_2$ overlayer, the result showed a sensitivity enhancement of 36.3% [13]. Most TMDCs modified SPR sensors were implemented with sophisticated prism structures and handled by angle-interrogation [14], [15]. There are few practical bio-sensing applications using optical fiber structures and wavelength-interrogation reported. Compared to other TMDCs materials, $MoSe_2$ has a larger layer spacing and a smaller energy band gap which will lead to better sensing performance [16]. It has been reported that the absorption capability is wavelength-dependent and the level of that for typical TMDCs materials is: $MoSe_2 < MoS_2$. Lower photon absorption is more beneficial to real-time sensing [17]. Therefore, the ability of materials aforementioned to enhance the detection sensitivity should be: $MoSe_2 > MoS_2$. In another word, $MoSe_2$ will perform better for enhancing the sensitivity of the sensor.

Besides the sensitivity, immobilizing biomolecules on the optical fiber for specific immunity is also significant. Methods of N-(3-Dimethylaminopropyl)-N'-Ethyl carbodiimide hydrochloride (EDC), N-Hydroxysuccinimide (NHS) and cross-linking agent have been applied to improve the immobilization efficiency [18]–[20]. However, these various chemical regents are time-consuming and can decrease the activity of biological recognition layer in the immunological reactions. One of the typical applications of the MoS_2 modified optical fiber biosensor was to detect the Escherichia coli [21]. The monoclonal antibodies and the optical fiber surface were connected by hydrophobic interactions, which was far behind the binding of functional groups. Consequently, developing an effective immobilization method remains a challenge. Cysteamine hydrochloride with abundant amino and sulfydryl groups can be employed to facilitate the immobilization [22]. Applying the functional groups in molecules or modifying the molecules to produce the self-assembled films should be investigated for further research.

In this work, the $MoSe_2$-Au based sensitivity enhanced optical fiber SPR biosensor was proposed, where the Cysteamine hydrochloride was employed as the linker to form the self-assemble film. Taking account of both the sensitivity and the figure of merit (FOM), we obtained the best deposition cycle of $MoSe_2$ layer. Simulations, biological affinity detection and immunization experiments with $MoSe_2$-Au optical fiber SPR biosensor were carried out. The performance and specificities of the fabricated biosensor were further evaluated and compared with other reported SPR biosensors. The results demonstrated a bright prospect of our developed optical fiber SPR biosensor for the protein detection and clinical diagnosis.

II. EXPERIMENTAL SETUP AND METHOD

A. EXPERIMENTAL SETUP

Optical fiber rotating magnetron sputtering coating instrument was applied to ensure the uniformity of deposited film. The experimental setup for SPR bio-sensing was illustrated in Fig. 1. The sensing system consisted of a tungsten halogen light source, the SPR biosensor with a glass tube, a spectrophotometer (HR 4000 from Ocean Optics Co.) with a range of 200-1100 nm and a resolution of 20 pm.

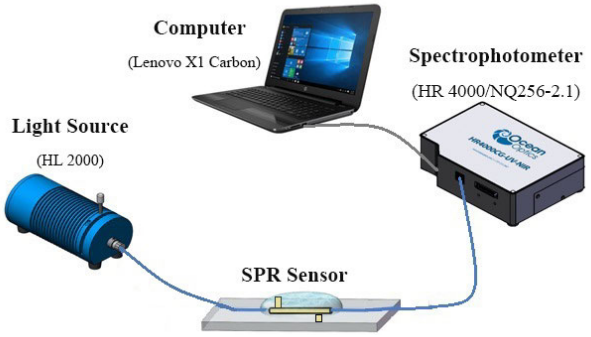

FIGURE 1. The experimental setup for optical fiber SPR sensing system.

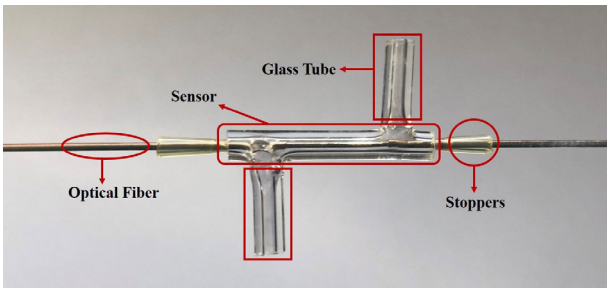

FIGURE 2. Physical map of home-made optical fiber SPR sensor.

A glass tube with upper and lower openings was used to prevent the evaporation of the solution and to ensure the coating time. The optical fiber was inserted into the glass tube and the two ends were blocked by self-made stoppers to prevent the leakage as Fig. 2.

B. MODEL OF THE SPR SENSING PLATFORM

The electromagnetic wave propagating in the optical waveguide enters the metal layer in the form of evanescent field and will excite the surface Plasmon wave. As the transverse component of the incident light k_x equals the propagation constant of the surface Plasmon wave β_{sp}, the SPR coupling condition is satisfied [23]:

$$\beta_{sp} = k_x \Rightarrow \sqrt{\frac{\varepsilon_m \varepsilon_s}{\varepsilon_m + \varepsilon_s}} = \sqrt{\varepsilon_0}\frac{\omega}{c}\sin\theta \tag{1}$$

where ω, c and θ characterize the angle frequency, the light speed in the vacuum and the incident angle, respectively. ε_m, ε_s and ε_0 represent the dielectric functions of the metal layer, the dielectric medium and the fiber core, respectively. Therefore, the basic elements of our SPR sensing platform consist of the metal layer and the sensing medium.

According to simulation results in our previous work, a larger diameter of optical fiber corresponded to a narrower resonance peak and a higher sensitivity [24]. However, the use of an overlarge core diameter will increase the cost of fiber

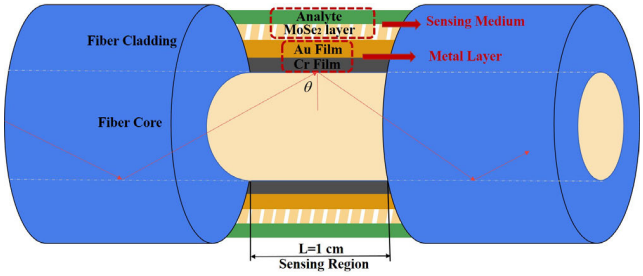

FIGURE 3. A schematic configuration of coated optical fiber SPR sensor.

and the difficulty of fiber to be connected to other optical components. Generally, the plastic multi-mode fiber with a core diameter of 600 μm was commonly used due to its easy accessibility and large contact reaction area. Its coating and cladding with the length of 1 cm in the middle region was removed using a sharp blade. The layer of chromium (5 nm) and gold (50 nm) were successively deposited on the sensing region using the vacuum sputtering coating instrument. The vacuum degree of deposition environment was 2×10^{-4} Pa. The sputtering angle was set to 80° and the working electric current was set to 100 mA. The thickness of each layer was calibrated by a crystal film thickness detector and the deposition rate of metal was experimentally determined.

After the step of the metal layer coating, the last step before the test experiment was the immobilization of the $MoSe_2$ layer. The completed sensor was immersed in the ultrasound-treated $MoSe_2$ isopropanol nano-dispersion (0.5 mg/mL) until the solution fully evaporated. The full evaporation of the nano-dispersion indicated the completion of one deposition cycle. The procedure of annealing at 50 °C for 5 hours was necessary to ensure the adhesion strength between the gold film and the $MoSe_2$ layer. Deposition cycles from 0 to 8 were all carried out by repeating the above evaporation process. Thus the model of optical fiber SPR sensing platform was composed of four layers including fiber core, metal layer, $MoSe_2$ layer and the analyte, where the latter two were regarded as the sensing medium. The configuration of the SPR sensor was schematically illustrated in Fig. 3.

C. SIMULATION RESULTS OF SPR SENSOR

The SPR sensor is sensitive to the refractive index (RI) of the surrounding environment. When the SPR phenomenon occurs, the resonance will absorb the energy and will cause the great losses of the signal intensity at the resonance wavelength, forming a trough in the transmission spectrum. To evaluate the RI sensitivity after adding $MoSe_2$, the transfer matrix method (TMM) of the multi-layer model [25] was employed and the corresponding simulations were carried out. The spectrum got broadened in the simulation results. It is found in Fig. 4(a) that the resonance wavelength had a red shift and the resonance peak became shallow, which demonstrated the transmission losses and the response changes after coating $MoSe_2$ layer. Fig. 4(b) shows the increase in the RI sensitivity of the sensor due to the use of $MoSe_2$. This can be

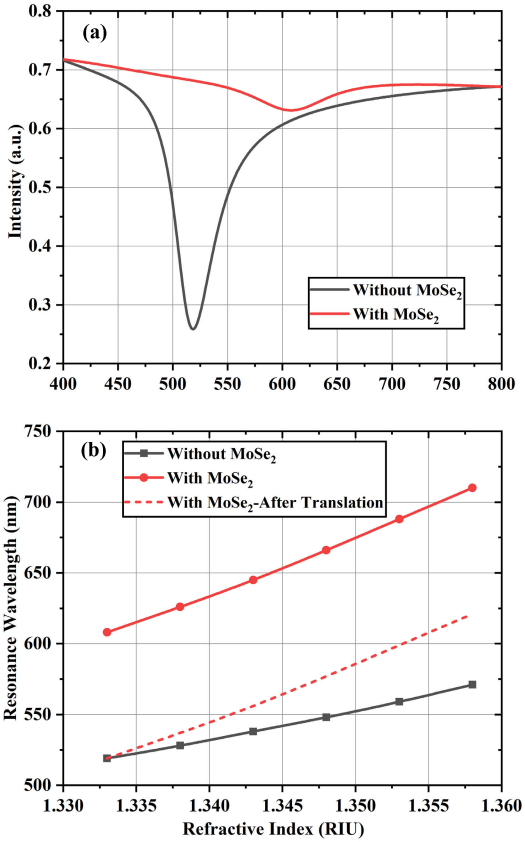

FIGURE 4. (a) Simulation results of spectral response, (b) Simulation results of RI sensitivity without and with $MoSe_2$ (For easy observation, the red dotted line is the curve after translation).

explained using the characteristics of the dielectric function, described as:

$$\varepsilon = \varepsilon' + \varepsilon'' i \tag{2}$$

where the real part ε' indicates the retained energy and the imaginary part ε'' represents the attenuation of the energy in the dielectric medium. The dielectric function of the metal layer is calculated using the Drude-Lorentz model, and the wavelength dependent dielectric function of the additional $MoSe_2$ material can be extracted accordingly [26]. The variation of the dielectric function in terms of the wavelength leads to the asymmetry of the SPR spectrum. In addition, the existence of $MoSe_2$ with a large real part ε' will absorb strong energy from the incident light and dramatically influence the sensor sensitivity. A large imaginary part ε'' will cause a significant attenuation of the electronic energy and will result in the broadening of the spectrum.

D. FUNCTIONALIZATION OF THE $MOSE_2$-AU BASED SPR BIOSENSOR

The 2 mM Cysteamine hydrochloride with an optimal concentration was functionalized on the optical fiber SPR sensor and was stored for 12 hours. In addition to generating the self-assemble film, the aminos ionized from the ammonium chloride in Cysteamine aggregated to form

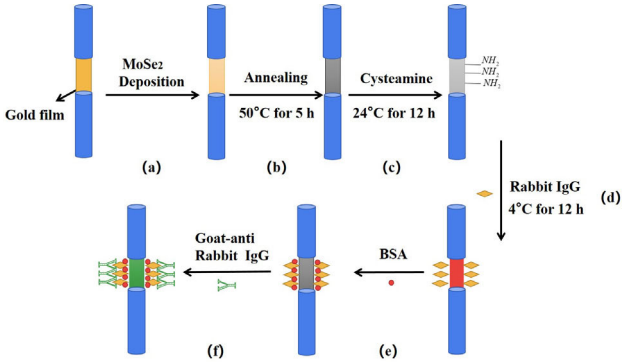

FIGURE 5. Schematic illustration of $MoSe_2$-Au film fabrication and modification for IgG immunoassay: (a) Gold film coated, (b) $MoSe_2$ deposition, (c) Formation of Cysteamine, (d) Rabbit IgG antigen modification, (e) Block of unbonded sites, (f) Binding interaction between Rabbit IgG and Goat-anti-Rabbit IgG.

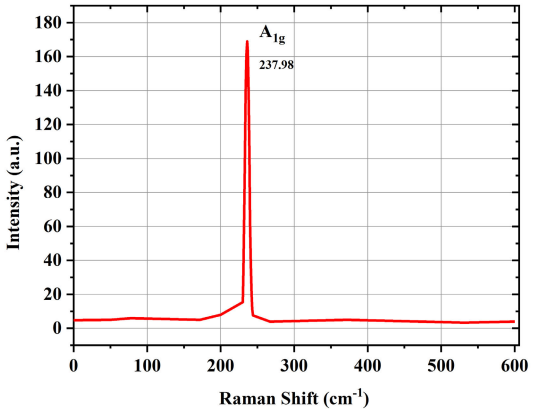

FIGURE 6. Roman spectrum of $MoSe_2$-Au optical fiber SPR sensor.

amino groups, which were positively charged to adsorb protein molecules. In order to investigate the bioaffinity of biosensor, the BSA solution (10 mg/mL) was used as the test protein and the best deposition cycles of $MoSe_2$ has been acquired. The manufactured $MoSe_2$-Au-Cystaemine based sensor was further modified using Rabbit IgG (1 mg/mL) for more than 20 hours at 4 °C (to prevent the protein inactivation). After the blocking of the unbound sites using the BSA, the $MoSe_2$-Au-Cystaemine-Rabbit IgG SPR biosensor was successfully produced for immunoassay. The diagram of immobilization procedures on the surface of the optical fiber was schematically shown in Fig. 5.

III. RESULTS AND DISCUSSION

A. CHARACTERIZATION

Raman spectroscopy is a practical tool to describe the properties of materials. The Raman spectrum of the $MoSe_2$-Au based optical fiber SPR sensor was shown in Fig. 6. An obvious peak was observed at the location of 237.8 cm^{-1}, indicating that the A_{1g} mode was derived from Se atoms oscillating around Mo atom [27].

Field-emission scanning electron microscopy (FESEM) was applied to characterize the surface morphology. Images and cross-sections of the optical fiber SPR sensor with pure

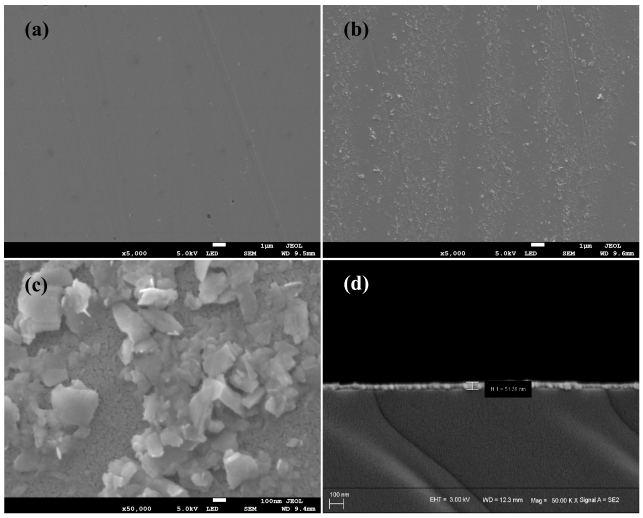

FIGURE 7. (a) SEM images of gold film optical fiber SPR sensor with magnification of 5000x, (b) SEM images of four layers of $MoSe_2$ functionalized optical fiber SPR sensor with magnification of 5000x, (c) 50000x, and (d) the thickness of four layers of $MoSe_2$.

gold film and four layers of $MoSe_2$ nano-film in different magnifications were shown in from Fig. 7(a) to Fig. 7(d).

The surface of the gold filmed optical fiber was smooth whereas the $MoSe_2$ coated surface observed visible nano-sheets structure. These characterization results demonstrate that the $MoSe_2$ material has been uniformly deposited on the surface of optical fiber and has provided a larger surface area for binding biological molecules and improving the performance of the sensor.

B. SENSITIVITY OF $MOSE_2$-AU BASED SPR SENSOR

The Au-based and the $MoSe_2$-Au based optical fiber SPR sensors were totally immersed in the RI solution in the range of 1.333-1.358 with an interval of 0.005. The normalized transmission spectra were shown in from Fig. 8(a) to Fig. 8(b).

When $MoSe_2$ was applied, the valley position of the spectrum shifted to a larger wavelength, accompanied with an obvious broadening in the full width at half minimum (FWHM). The resonance wavelength of the $MoSe_2$-Au based sensor has a red shift of 60.05 nm, which was double of that for the gold filmed sensor with a red shift of 30.51 nm. The sensitivity of refractive index is expressed as S:

$$S = \delta\lambda/\delta n \tag{3}$$

where δn describes the change of RI, and $\delta\lambda$ represents the corresponding shift of the resonance wavelength. To quantitatively analyze the performance of the sensors with and without the use of $MoSe_2$, the linear relationships between RI and the resonance wavelength were fitted in Fig. 9(a). The maximum sensitivity was 2821.81 nm/RIU, roughly 98.7% higher than that of the previous SPR sensor with gold film only (1420.44 nm/RIU). It can be seen that the RI sensitivity enhances with the introduction of $MoSe_2$, which is in accordance with the simulation results.

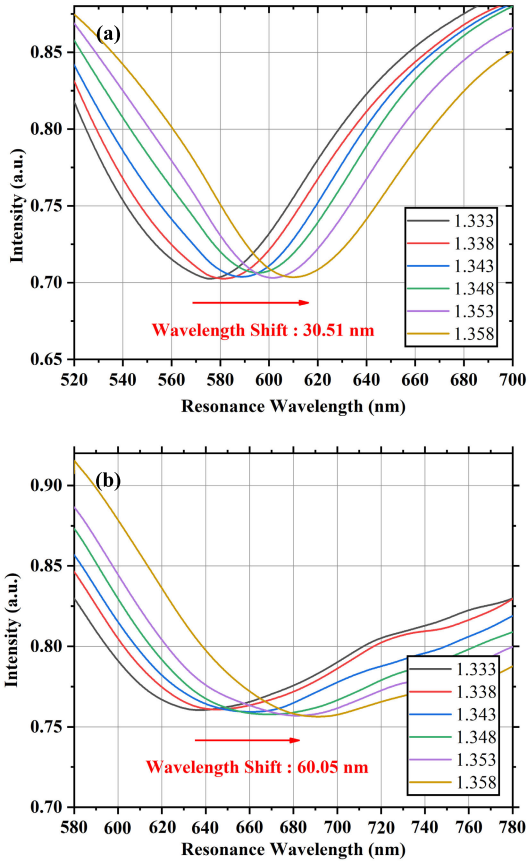

FIGURE 8. Real-time spectral response to the refractive index change of optical fiber SPR sensor (a) without $MoSe_2$ and (b) with $MoSe_2$.

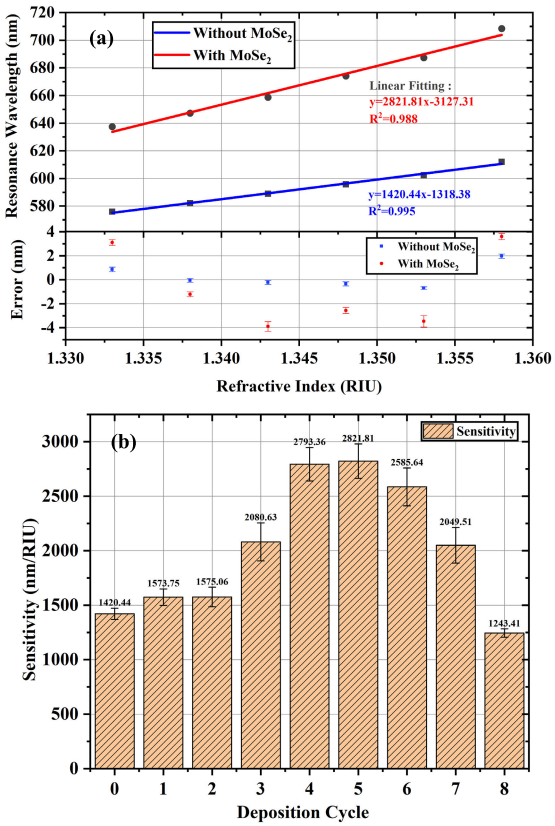

FIGURE 9. (a) Linear fitting of optical fiber SPR sensor without and with $MoSe_2$, (b) RI Sensitivity of $MoSe_2$-Au optical fiber SPR sensor with different deposition cycles from 0 to 8.

In order to obtain the impact of the thickness, we tested the RI sensitivity of $MoSe_2$-Au based sensors with the deposition cycles from 0 to 8. The RI sensitivity increased significantly from 0 to 5 and then decreased gradually from 5 to 8, as shown in Fig. 9(b).

It can be explained from the aspects of the effective refractive index and the evanescent field. The introduction of the $MoSe_2$ actually transforms the sensing medium into the synthetic structure using the $MoSe_2$ nano-film and the analyte layer. The relationship between the increment of the refractive index Δn_d and the layer thickness h can be written as [28]:

$$\Delta n_d = (dn/dc)_v \, \Delta\Gamma / h \tag{4}$$

where $(dn/dc)_v$ represents the RI to the concentration of analyte, $\Delta\Gamma$ indicates the relative concentration of the combination. $MoSe_2$ is regarded as the target combination in this case and the constant deposition will increase $\Delta\Gamma$ with a higher proportion of $MoSe_2$, the given RI solution makes the fixed value of $(dn/dc)_v$. Then Δn_d increases correspondingly according to (4), which leads to a larger shift of resonance wavelength and improvement of RI sensitivity. However, the deposition increases the thickness of the layer and also reduces the overlap between the analyte layer and the evanescent field. When the second factor occupies, the SPR phenomenon becomes weak and the sensitivity will decrease with the increase of the thickness of $MoSe_2$. Therefore, the sensitivity climbs first and then decreases. This can be clearly analyzed by the interactions between the two above effects, which is consistent with the experimental results.

TABLE 1. The FOM and the RSD of RI sensitivity with different deposition cycles.

Layer	0	1	2	3	4	5	6	7	8
FOM (RIU^{-1})	28.01	31.48	31.50	32.01	37.24	28.26	25.86	21.15	7.52
RSD (%)	3.65	4.79	5.71	8.40	5.49	5.60	6.71	8.01	3.09

Considering the fact that the $MoSe_2$ layer improved the sensitivity while increased the FWHM, the detection accuracy of the sensor could be reduced. Therefore, the figure of merit defined as $FOM = S/FWHM$ is employed to investigate the performance of sensor comprehensively. The FWHM was calculated by Matlab with the process of scanning spectrum data, extracting the baseline and achieving the half peak value. The relative standard deviation (RSD) of the RI sensitivity with different deposition cycles and the averaged FOM of the $MoSe_2$-Au based optical fiber SPR sensor were given in Table 1. Therefore, the best deposition cycle was found to be 4 with the RI sensitivity of 2793.36 nm/RIU and the FOM of 37.24 RIU^{-1}. Furthermore, the FOM value can

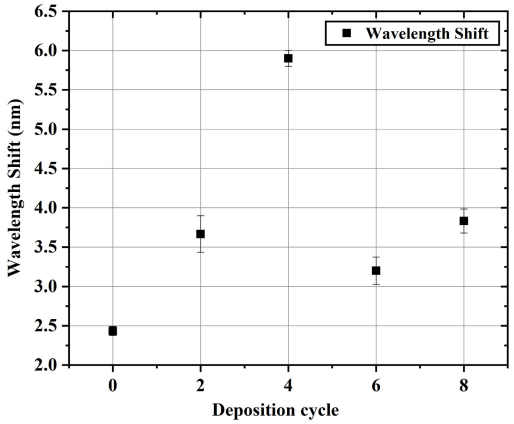

FIGURE 10. The wavelength shift of optical fiber SPR biosensor (deposition cycles from 0 to 8) with a concentration of 10 mg/mL BSA solution.

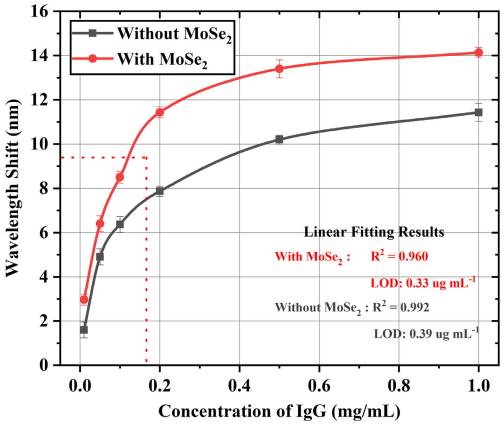

FIGURE 11. Response curve with different concentrations of Goat-anti-Rabbit IgG (Inside the dotted area is the linear region).

be increased by introducing the modulation layer. Adding Si material with high real part and low imaginary part of the dielectric function has been reported to modify the sensitivity and FWHM [29], further enhances the FOM value of the traditional gold filmed SPR sensor.

C. BIOAFFINITY EVALUATION OF $MOSE_2$-AU BASED SPR BIOSENSOR

BSA, also known as the fifth component, is a kind of albumin in bovine serum with an appropriate molecular weight. It is widely used in biochemical experiments and it can effectively prevent non-specific adsorptions. The bioaffinity detection was performed using BSA (10 mg/mL), to make preparations for next immunization experiments. To ensure the repeatability of experiments, several groups of repetitive experiments were carried out and the wavelength shifts with $MoSe_2$ deposition cycles from 0 to 8 were plotted in Fig. 10.

The $MoSe_2$-Au based SPR biosensor provided a maximum shift of 5.8 nm at the deposition cycle of 4. The sensitivity increases first and then decreases. This can also be explained using (4), where the BSA is the analyte with a fixed concentration. In other words, as BSA accumulates and the thickness of $MoSe_2$ increases, the ionization intensity of the evanescent field is not strong enough to break down the dielectric medium and to excite the SPR phenomenon.

D. DETERMINATION OF ANTIBODY-ANTIGEN SPECIFIC BINDING

The above sensitivity and the bioaffinity experiments have determined the optimum deposition cycle of $MoSe_2$, so we chose four layers to carry out the immunization experiment. After the procedure of coating Cysteamine hydrochloride (2 mM) and Rabbit IgG (1 mg/mL), the modified SPR biosensor was exposed to Goat-anti-Rabbit IgG solutions with different concentrations (0.01, 0.025, 0.05, 0.1, 0.2, 0.5, 1 mg/mL at 37°C) to detect specific binding. The comparative experiments were performed using the Au-based SPR biosensor by the same strategy and measurement data were recorded in Fig. 11.

TABLE 2. Comparison among proposed SPR sensor with other existing sensors.

Analyte	Method	LOD	Reference
Human IgG	PSAMs and PSS	1.75	[30]
Horse IgG	Dopamine-AuNPs	0.625	[31]
Mouse IgG	Ag-Nanocubes	0.6	[32]
Goat-anti-Huamn IgG	Polydopamine-Au film	0.9	[33]
Anti-Human IgG	GNS and GNR	1.6	[34]
Goat-anti-Rabbit IgG	$MoSe_2$-Au film	0.33	This Work

Note: PSAMs mean the polyelectrolyte self-assembled multi-layers, PSS means the diallyldimethyl ammonium chloride, GNS represent the gold nanoparticles and GNR are the gold nanocubes.

The curves rose in the linear region within the range of 0.01-0.1 mg/mL, then reached the optimum concentration and finally got saturated. The wavelength shift illustrated better biological characteristics of $MoSe_2$, leading to the improvement of the sensing performance. The limit of detection (LOD) is also applied to evaluate the properties of biosensor. The LOD can be defined as:

$$LOD = \Delta\lambda / S_b \tag{5}$$

where $\Delta\lambda$ represents the resolution of the spectrophotometer (20 pm) and S_b is the sensitivity of bio-sensing. Noticeably, S_b corresponds to the slope of the biological interaction curve in our experiment. After the calculation, the LOD of $MoSe_2$-Au based optical fiber SPR biosensor was 0.33 μg/mL which was roughly 18.2% better compared to the sensor without the use of $MoSe_2$ (0.39 μg/mL). Table 2 listed the comparison of the LOD values between the proposed sensor and other reported SPR biosensors. The Polydopamine-modified SPR biosensor was developed to detect IgG solution and LOD value of 0.625 μg/mL was obtained. Moreover, various nanostructures including gold nanoparticles and gold nanocubes were reported for enhancing the sensitivity of SPR biosensor, which demonstrated the good bio-sensing properties and obtained the LOD of 1.6 μg/mL. By contrast, the $MoSe_2$-Au optical fiber SPR biosensor developed in our study exhibited a better performance.

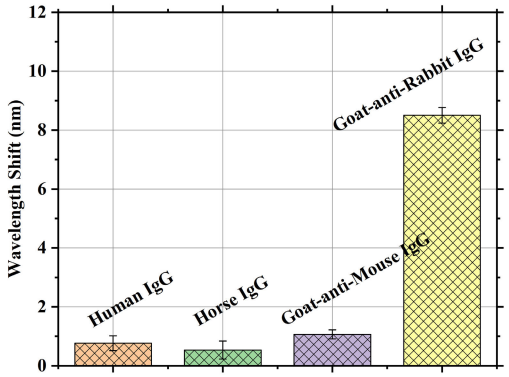

FIGURE 12. Shift of the resonance wavelength measured with different solution of 100μg/mL based on the $MoSe_2$-Au optical fiber SPR biosensor.

On the one hand, the large surface area of $MoSe_2$ increases the binding density of antibodies, and its high carrier mobility results in the capture of more target analyte. On the other hand, the Cysteamine hydrochloride with abundant amino groups are enabled to gather considerable protein molecules. Furthermore, it can form a self-assembled film to link the optical fiber tightly. Our design demonstrated that the combination of $MoSe_2$ and Cysteamine hydrochloride can significantly improve the properties of conjugates and enhance the performance of the optical fiber biosensor.

E. SPECIFICITY OF $MOSE_2$-AU BASED SPR BIOSENSOR

To evaluate the specificity of the $MoSe_2$-Au based optical fiber SPR biosensor, various solutions (Human IgG, Horse IgG, Rabbit-anti-Mouse IgG and Goat-anti-Rabbit IgG) were applied to detect the binding efficiency. The Rabbit IgG was also adopted as the immobilized antigen and the protein solution with a concentration of 100 μg/mL were dripped sequentially as the comparative experiments. As shown in Fig. 12, only the Goat-anti-Rabbit IgG one obtained the distinct shift, and this demonstrated the optimum specificity of $MoSe_2$-Au based biosensor. Most cancer markers for immunoreaction such as carcinoembryonic antigen (CEA) and prostate specific antigen (PSA) are mostly protein molecules, and they can be specifically detected by our proposed label-free biosensor. This shows a strong applicability of the proposed optical fiber SPR biosensor for disease diagnosis and immunization therapy.

IV. CONCLUSION

In this paper, the optical fiber SPR biosensor with the $MoSe_2$-Au structure was developed and experimentally investigated. The refractive index sensitivity of $MoSe_2$-Au modified optical fiber SPR sensor reached 2821.81 nm/RIU, which was nearly 98.7% higher than that of conventional sensors without using $MoSe_2$. Meanwhile, a maximum redshift was acquired at the best deposition cycle of 4 in the BSA bioaffinity experiment. The limit detection of 0.33 μg/mL was also obtained in antigen-antibody interactions, which was 18.2% better than the gold filmed biosensor. The results demonstrated the feasibility and specificity of our proposed $MoSe_2$-Au optical fiber SPR biosensor. Furthermore, this work provided a bio-analytical miniaturized platform for biosensing with the real-time detection, high sensitivity and great applicability in immunoassay.

REFERENCES

[1] D. Daems, W. Pfeifer, I. Rutten, B. Sacca, D. Spasic, and J. Lammertyn, "Three-dimensional DNA origami as programmable anchoring points for bioreceptors in fiber optic surface plasmon resonance biosensing," *ACS Appl. Mater. Interfaces*, vol. 10, no. 28, pp. 23539–23547, Jul. 2018.
[2] M. Loyez, J. C. Larrieu, S. Chevineau, M. Remmelink, D. Leduc, and B. Bondue, "*In situ* cancer diagnosis through online plasmonics," *Biosens. Bioelectron.*, vol. 131, pp. 104–112, Apr. 2019.
[3] J.-F. Masson, "Surface plasmon resonance clinical biosensors for medical diagnostics," *ACS Sensors*, vol. 2, no. 1, pp. 16–30, Jan. 2017.
[4] A. Jabin, K. Ahmed, M. Rana, B. Paul, B. K. Luo, and V. Dhasarathan, "Titanium-coated dual-core D-shaped SPR-based PCF for hemoglobin sensing," *Plasmonics*, vol. 14, no. 6, pp. 1601–1610, Apr. 2019.
[5] A. Jabin, K. Ahmed, M. Rana, B. K. Paul, V. Dhasarathan, and M. S. Uddin, "Multicore bi-layer gold-coated SPR-based sensor for simultaneous measurements of CFC and HCFC," *Int. J. Mod. Phys. B*, vol. 33, no. 27, Apr. 2019, Art. no. 1950316.
[6] I. S. Amiri, B. K. Paul, K. Ahmed, K. Aly, R. Zakaria, P. Yupapin, and D. Vigneswaran, "Tri-core photonic crystal fiber based refractive index dual sensor for salinity and temperature detection," *Microw. Opt. Technol. Lett.*, vol. 61, no. 3, pp. 847–852, Jul. 2018.
[7] M. Khana, K. Ahmed, M. Hossaina, B. K. Paul, T. Nguyen, and V. Dhasarathan, "Exploring refractive index sensor using gold coated D-shaped photonic crystal fiber for biosensing applications," *Optik*, vol. 202, Oct. 2019, Art. no. 163649.
[8] S. Jiang, Z. Li, C. Zhang, S. Gao, Z. Li, and H. Qiu, "A novel U-bent plastic optical fibre local surface plasmon resonance sensor based on a graphene and silver nanoparticle hybrid structure," *J. Phys. D, Appl. Phys.*, vol. 50, no. 16, Apr. 2017, Art. no. 165105.
[9] H.-Q. Liang, B. Liu, and J.-F. Hu, "An ultra-highly sensitive surface plasmon resonance sensor based on D-shaped optical fiber with a silver-graphene layer," *Optik*, vol. 149, pp. 149–154, Sep. 2017.
[10] Y. V. Morozov and M. Kuno, "Optical constants and dynamic conductivities of single layer MoS_2, $MoSe_2$, and WSe_2," *Appl. Phys. Lett.*, vol. 107, no. 8, Aug. 2015, Art. no. 083103.
[11] E. Torun, H. Sahin, S. Cahangirov, A. Rubio, and F. M. Peeters, "Anisotropic electronic, mechanical, and optical properties of monolayer WTe_2," *J. Appl. Phys.*, vol. 119, no. 7, Feb. 2016, Art. no. 074307.
[12] M. S. Rahman, S. Anower, R. Hasan, B. Hossain, and M. I. Haque, "Design and numerical analysis of highly sensitive Au-MoS_2-graphene based hybrid surface plasmon resonance biosensor," *Opt. Commun.*, vol. 396, pp. 36–43, Aug. 2017.
[13] Y. Luo, S. Hu, H. Wang, Y. Chen, J. Dong, and Z. Jiang, "Sensitivity-enhanced surface plasmon sensor modified with $MoSe_2$ overlayer," *Opt. Express*, vol. 26, no. 26, pp. 34250–34258, Dec. 2018.
[14] M. S. Rahman, M. R. Hasan, K. A. Rikta, and M. S. Anower, "A novel graphene coated surface plasmon resonance biosensor with tungsten disulfide (WS_2) for sensing DNA hybridization," *Opt. Mater.*, vol. 75, pp. 567–573, Jan. 2018.
[15] H. Wang, H. Zhang, J. Dong, S. Hu, W. Zhu, and W. Qiu, "Sensitivity-enhanced surface plasmon resonance sensor utilizing a tungsten disulfide (WS_2) nanosheets overlayer," *Photon. Res.*, vol. 6, no. 6, pp. 485–491, Jun. 2018.
[16] I. Abid, A. Bohloul, S. Najmaei, C. Avendano, H. L. Liu, and R. Pechou, "Resonant surface plasmon-exciton interaction in hybrid MoSe2@Au nanostructures," *Nanoscale*, vol. 8, no. 15, pp. 8151–8159, Apr. 2016.
[17] J. B. Maurya, A. François, and Y. K. Prajapati, "Two-dimensional layered nanomaterial-based one-dimensional photonic crystal refractive index sensor," *Sensors*, vol. 18, no. 3, p. 857, Mar. 2018.
[18] J. Ashley, M. Piekarska, C. Segers, L. Trinh, T. Rodgers, and R. Willey, "An SPR based sensor for allergens detection," *Biosens. Bioelectron.*, vol. 88, pp. 109–113, Feb. 2017.
[19] N. A. S. Omar, Y. W. Fen, J. Abdullah, M. H. M. Zaid, W. M. E. M. M. Daniyal, and M. A. Mahdi, "Sensitive surface plasmon resonance performance of cadmium sulfide quantum dots-amine functionalized graphene oxide based thin film towards dengue virus E-protein," *Opt. Laser Technol.*, vol. 114, pp. 204–208, Jun. 2019.

[20] Q. Wang and B.-T. Wang, "Surface plasmon resonance biosensor based on graphene oxide/silver coated polymer cladding silica fiber," *Sens. Actuators B, Chem.*, vol. 275, pp. 332–338, Dec. 2018.
[21] S. Kaushik, U. K. Tiwari, S. S. Pal, and R. K. Sinha, "Rapid detection of escherichia coli using fiber optic surface plasmon resonance immunosensor based on biofunctionalized molybdenum disulfide (MoS_2) nanosheets," *Biosens. Bioelectron.*, vol. 126, pp. 501–509, Feb. 2019.
[22] Q. Jiang, M. Xue, P. Liang, C. Zhang, J. Lin, and J. Ouyang, "Principle and experiment of protein detection based on optical fiber sensing," *Photon. Sens.*, vol. 7, no. 4, pp. 317–324, Dec. 2017.
[23] A. K. Sharma and B. D. Gupta, "Absorption-based fiber optic surface plasmon resonance sensor: A theoretical evaluation," *Sens. Actuators B, Chem.*, vol. 100, no. 3, pp. 423–431, May 2004.
[24] T. Wang, T. Liu, K. Liu, J. Jiang, L. Yu, and M. Xue, "An EMD-based filtering algorithm for the fiber-optic SPR sensor," *IEEE Photon. J.*, vol. 8, no. 3, pp. 1–8, Jun. 2016.
[25] B. Meshginqalam and J. Barvestani, "Performance enhancement of SPR biosensor based on phosphorene and transition metal dichalcogenides for sensing DNA hybridization," *IEEE Sensors J.*, vol. 18, no. 18, pp. 7537–7543, Sep. 2018.
[26] Q. Ouyang, S. Zeng, L. Jiang, L. Hong, G. Xu, and X. Q. Dinh, "Sensitivity enhancement of transition metal dichalcogenides/silicon nanostructure-based surface plasmon resonance biosensor," *Sci. Rep.*, vol. 6, Jun. 2016, Art. no. 28190.
[27] S. S. P. Nathamgari, S. Dong, E. Hosseinian, L. J. Lauhon, and H. D. Espinosa, "An experimental setup for combined *in-vacuo* Raman spectroscopy and cavity-interferometry measurements on TMDC nano-resonators," *Exp. Mech.*, vol. 59, no. 3, pp. 349–359, Mar. 2019.
[28] H. H. Nguyen, J. Park, S. Kang, and M. Kim, "Surface plasmon resonance: A versatile technique for biosensor applications," *Sensors*, vol. 15, no. 5, pp. 10481–10510, May 2015.
[29] Q. Ouyang, S. W. Zeng, J. Li, Y. H. Li, G. X. Xu, X. Dinh, J. Qian, S. L. He, J. L. Qu, C. Philippe, and K.-T. Yong, "Sensitivity enhancement of transition metal dichalcogenides/silicon nanostructure-based surface plasmon resonance biosensor," *Sci. Rep.*, vol. 6, pp. 1–13, Jun. 2016.
[30] Y. Zheng, T. Lang, B. Cao, J. Jin, R. Dong, and H. Feng, "Fiber optic SPR sensor for human Immunoglobulin G measurement based on the MMF-NCF-MMF structure," *Opt. Fiber Technol.*, vol. 46, pp. 179–185, Dec. 2018.
[31] N. Wang, D. Zhang, X. Deng, Y. Sun, X. Wang, and P. Ma, "A novel surface plasmon resonance biosensor based on the PDA-AgNPs-PDA-Au film sensing platform for horse IgG detection," *Spectrochimica Acta A*, vol. 191, pp. 290–295, Feb. 2018.
[32] D. Zhang, Y. Sun, Q. Wu, P. Ma, H. Zhang, and Y. Wang,"Enhancing sensitivity of surface plasmon resonance biosensor by Ag nanocubes/chitosan composite for the detection of mouse IgG," *Talanta*, vol. 146, pp. 364–368, Jan. 2016.
[33] S. Shi, L. Wang, R. Su, B. Liu, R. Huang, and W. Qi, "A polydopamine-modified optical fiber SPR biosensor using electroless-plated gold films for immunoassays," *Biosensors Bioelectron.*, vol. 74, pp. 454–460, Dec. 2015.
[34] J. Cao, M. H. Tu, T. Sun, and K. T. V. Grattan, "Wavelength-based localized surface plasmon resonance optical fiber biosensor," *Sens. Actuators B, Chem.*, vol. 181, pp. 611–619, May 2013.

KUN LIU received the B.Eng. degree in opto-electronics information engineering and the M.Eng. and Ph.D. degrees in optical engineering from Tianjin University, Tianjin, China, in 2004, 2006, and 2009, respectively. From 2009 to 2010, he worked as a Postdoctoral Researcher at Tianjin University, where he is currently a Professor with the College of Precision Instruments and Optoelectronic Engineering. His research interests include the development of physics and chemistry sensing systems based on optical fiber lasers.

JIAHANG ZHANG received the B.E. degree from the Changchun University of Science and Technology, China, in 2018. She is currently pursuing the M.S. degree with Tianjin University. Her research interests include fiber sensing, surface plasmon resonance sensor, and gas sensing.

JUNFENG JIANG received the B.S. degree from the Southwest Institute of Technology, Mianyang, China, in 1998, and the M.S. and Ph.D. degrees from Tianjin University, Tianjin, China, in 2001 and 2004, respectively. He is currently a Professor with Tianjin University. His research interests include fiber sensors and optical communication performance measurement.

TIANHUA XU received the B.Eng., M.Sc., and Ph.D. degrees from Tianjin University, China, in 2005, 2007, and 2011, respectively, and the second Ph.D. degree from the KTH Royal Institute of Technology, Sweden, in 2012. He is currently a Professor with Tianjin University, China. His research interests include optical communications and fiber sensing.

SHUANG WANG was born in Tianjin, China, in 1982. She received the M.S. degree from the College of Computer Science and Technology, Shandong University, Shandong, China, in 2005, and the Ph.D. degree in optics from Tianjin University, Tianjin, China, in 2014. She is engaged in the research of optical fiber sensing technology, photoelectric detection technology, and other fields.

PENGXIANG CHANG was born in Shandong, China, in 1990. He received the B.Eng. degree in applied physics from the Hefei University of Technology, China, in 2013, and the M.Eng. degree in plasma physics from the University of Chinese Academy of Sciences, Beijing, China, in 2015. He is currently pursuing the Ph.D. degree in optical engineering with Tianjin University, Tianjin, China. His research interest mainly focuses on surface plasma resonance fiber sensing.

ZHAO ZHANG received the B.Eng. from Xi'an Technological University, China, in 2014, and the M.S. degree from the Beijing University of Technology, China, in 2017. He is currently pursuing the Ph.D. degree in optical engineering with the Tianjin University. His research interests are surface plasmon resonance sensor and two-dimensional materials sensing.

JINYING MA received the B.S. and M. S. degrees from Tianjin University, China, in 2006 and 2017, respectively, where she is currently pursuing the Ph.D. degree. Her research interests include fiber sensing and surface plasmon resonance sensor.

TIEGEN LIU received the B.Eng., M.Eng., and Ph.D. degrees from Tianjin University, China, in 1982, 1987, and 1999, respectively. He is currently a Professor with Tianjin University. His research interests include photoelectric detection and fiber sensing. He is a Chief Scientist of the National Basic Research Program of China under Grant 2010CB327802.